

Hydrodynamic Instability of the Flux-antiflux Interface in Type-II Superconductors

L.M. Fisher

*All-Russian Electrical Engineering Institute, 12 Krasnokazarmennaya Street, 111250 Moscow,
Russian Federation*

P.E. Goa, M. Baziljevich, T.H. Johansen

Department of Physics, University of Oslo, P.O. Box 1048, Blindern, 0316 Oslo 3, Norway

A.L. Rakhmanov

*Institute for Theoretical and Applied Electrodynamics Russian Academy of Science, 13/19
Izhorskaya Street, 127412 Moscow, Russian Federation*

V.A. Yampol'skii

*Institute for Radiophysics and Electronics Ukrainian Academy of Science, 12 Proskura Street,
61085 Kharkov, Ukraine*

Abstract

The macroturbulence instability observed in fluxline systems during remagnetization of superconductors is explained. It is shown that when a region with flux is invaded by antiflux the interface can become unstable if there is a relative tangential flux motion. This condition occurs at the interface when the viscosity is anisotropic, e.g., due to flux guiding by twin boundaries in crystals. The phenomenon is similar to the instability of the tangential discontinuity in classical hydrodynamics. The obtained results are supported by magneto-optical observations of flux distribution on the surface of a YBCO

single crystal with twins.

The interest in the physics of the vortex state in type-II superconductors increased significantly after the discovery of high- T_c superconductivity (HTS). A main reason for the renewed attention is the observation of many novel nontrivial phenomena occurring in the vortex matter of the HTS materials. The perhaps most dramatic of these phenomena is the turbulence instability of the vortex-antivortex interface, which was observed in 1–2–3 systems using magneto-optical (MO) imaging [1–3]. It consists in the following. When magnetic flux is trapped in the superconductor and a moderate field of reverse direction is subsequently applied, a boundary of zero flux density will separate regions containing flux and antflux. In some temperature and field range this flux-antiflux distribution can display unstable behavior characterized by an irregular propagation of the boundary where finger-like patterns develop. This contrasts strongly the regular propagation of the flux front during virgin field penetration, when only one flux polarity is present in the sample. It is clear that the instability, often called macroturbulence in the literature, cannot be understood within the frameworks of the critical state model or conventional models for flux relaxation [4,5].

An attempt to explain this remarkable behavior of the flux-antiflux interface was made in [6], where the instability was attributed to a thermal wave generated by local heat release in the vortex-antivortex annihilation. Unfortunately, this mechanism can hardly be accepted. Indeed, the vortex energy consists of two terms, where one is the magnetic part related to the magnetic field of the vortices. The other part is stored within the vortex core and represents the condensation energy. The magnetic energy of a vortex-antivortex pair is dissipated as Joule heat as they are getting close to each other, but before the annihilation takes place. This energy, which equals $\vec{J}\vec{E}$ where \vec{J} is the current density and \vec{E} is the electric field generated by the vortex motion, is dissipates not only at the interface, but in the bulk of the sample. Hence, only the release of the core energy in the process of annihilation is concentrated near the interface. A simple calculation shows that the core energy is much smaller than the magnetic part and will cause only a negligible rise of the sample temperature [7], thereby ruling out that thermal effects are responsible for the instability.

In this Letter we present an explanation focussing on the experimental fact that the instability was reported only for $\text{YBa}_2\text{Cu}_3\text{O}_{7-\delta}$ and other 1–2–3 single crystals. These materials are characterized by the existence of two twin boundary systems oriented orthogonally to each other in the **ab** plane. The vortex motion in such crystals is governed by a pronounced guiding effect [8,9], and the viscosity coefficient for motion along the twin boundaries should be much smaller than across them. This anisotropy gives rise to vortex motion with a velocity component normal to the Lorentz force. The vortices and antivortices are then forced to move towards each other along the interface, where the tangential component of the velocity becomes discontinuous. It is well known that hydrodynamical flow under such conditions can be unstable [10], and we show here that a purely hydrodynamic theory of the vortex-antivortex system with anisotropic viscosity can explain the origin of the macroturbulence.

Consider an infinite superconducting plate of thickness $2d$ with the external magnetic field \vec{H} oriented parallel to the sample surface along the z -axis. The x -axis is perpendicular to the plate and $x = 0$ in the center. Let H first increase and then be lowered through zero to a negative value. Then two kinds of vortices will exist in the sample; one with field direction along the positive z -axis (*vortices*) and one directed oppositely (*antivortices*). From the symmetry of the problem it is sufficient to consider only the region $0 < x < d$, and Fig. 1 shows schematically the distributions $N_1(x)$ and $N_2(x)$ of vortex and antivortex densities.

The densities N_1 and N_2 satisfy the continuity equation,

$$\frac{\partial N_\alpha}{\partial t} + \text{div}(N_\alpha \vec{V}_\alpha) = 0, \quad \alpha = 1, 2 \quad (1)$$

where \vec{V}_α are the vortex and antivortex velocities. In the regime of anisotropic viscous flow they are related to the Lorentz driving force by,

$$\eta_{ik} N_\alpha V_{\alpha k} = F_{Li}, \quad \vec{F}_L = \frac{1}{c} \vec{B} \times \vec{J}, \quad (2)$$

$$\vec{B} = N_\alpha \vec{\Phi}_0, \quad \vec{J} = \frac{c}{4\pi} \nabla \times \vec{B}.$$

Here η_{ik} is the symmetrical tensor of the anisotropic viscosity and Φ_0 is the magnetic flux quantum. Eq. (2) can be rewritten as,

$$V_{\alpha i} = -\frac{\Gamma\Phi_0^2}{4\pi}\gamma_{ik}\frac{\partial N_{\alpha}}{\partial x_k}, \quad (3)$$

where γ_{ik} is the dimensionless tensor of the inverse viscosity, $\eta_{ik}^{-1} = \Gamma\gamma_{ik}$, and the coefficient Γ is chosen so that the principal values of γ_{ik} are unity and ε , which satisfies $0 < \varepsilon < 1$. The case of a strong guiding effect corresponds to $\varepsilon \rightarrow 0$. Note that Γ increases rapidly with the temperature due to thermal depinning of the vortices.

To solve the problem one must also formulate boundary conditions at the vortex-antivortex interface. Generally the position of the interface, $x = x_0$, depends on the y -coordinate and time t as it moves with a velocity \vec{U} . The first condition is that the total flux of vortices and antivortices through the interface vanishes,

$$N_1(\vec{V}_1 - \vec{U})_n + N_2(\vec{V}_2 - \vec{U})_n = 0. \quad (4)$$

Secondly, both vortex polarities annihilate at the interface with the rate proportional to the product of their densities,

$$N_1(\vec{V}_1 - \vec{U})_n = RN_1N_2. \quad (5)$$

The parameter R can depend on the vortex densities and velocities but, for simplicity, we assume here that it is a phenomenological constant. A similar model for the annihilation process was used in Ref. [6]. However, contrary to [6], we consider the parameter R to be defined by the microscopic Meissner current of individual vortices, which is much greater than the macroscopic currents J . Therefore, the relative velocity of annihilating vortices and antivortices is much greater than the hydrodynamic velocity V_{α} . As a result, the region where vortices and antivortices coexist and annihilation takes place is very narrow, and can be represented by the surface $x = x_0(y, t)$. Finally, we take the magnetic induction to be zero, i. e.,

$$N_1 = N_2, \quad (6)$$

at $x = x_0(y, t)$. This condition is also a direct consequence of Eq. (4) if the vortex and antivortex densities on the interface were equal to zero initially.

As a first step, we determine what the model predicts for the unperturbed distribution profiles N_1 and N_2 . In this case the vortex-antivortex interface is the plane $x = x_0(t)$ which moves with the velocity $U = dx_0(t)/dt$. Since a simple solution with constant $U \neq 0$ could not be found, we consider only the stationary profile with $U = 0$. With $\partial N_1/\partial t = \partial N_2/\partial t = 0$, the Eqs. (1), (4)–(6) give,

$$N_1(x) = N_2(d) \left(\frac{x_0 + d/2r - x}{d + d/2r - x_0} \right)^{1/2},$$

$$N_2(d) = H_0/\Phi_0, \tag{7}$$

$$N_2(x) = N_2(d) \left(\frac{x + d/2r - x_0}{d + d/2r - x_0} \right)^{1/2}, \quad r = \frac{4\pi R d}{\Gamma \Phi_0^2 \gamma_{xx}}.$$

In the following, we assume $r \gg 1$ since the rate of the annihilation is fast and the viscosity is not small. Therefore, at the interface the vortex densities are relatively small, $N_1 = N_2 \sim N_2(d)r^{-1/2}$ while the spatial derivatives of N_1 and N_2 at $x = x_0$ are large,

$$N_2' = -N_1' = N_1 r/d, \quad N_2'' = N_1'' = -N_1(r/d)^2. \tag{8}$$

Then, also the velocities $V_{\alpha x, y}(x = x_0)$ are relatively high, since they are proportional to $r^{1/2}$ near the interface.

If one cannot provide fixed values of the vortex and antivortex densities $N_1(0)$ and $N_2(d)$ at the boundaries, the discussed stationary profiles cannot be realized. In practice the external magnetic field defines the density of the antivortices only. Because of this asymmetry and the vortex-antivortex annihilation, the total number of the vortices will decrease with time and the interface moves towards the middle of the sample. To simplify the problem, we assume the interface velocity U to be much smaller than the vortex velocity V_α , i. e. we consider the problem in the quasi-stationary regime.

To investigate the stability of the interface with respect to small perturbations, it is suitable to introduce the following dimensionless variables,

$$\begin{aligned}
n_\alpha &= N_\alpha/N_\alpha(x_0), \quad \tau = t/t_0, \quad t_0 = \frac{\Gamma\Phi_0^2\gamma_{xx}}{4\pi R^2 N_\alpha(x_0)}, \\
\xi &= x/L, \quad \zeta = y/L, \quad L = \frac{\Gamma\Phi_0^2\gamma_{xx}}{4\pi R} = d/r.
\end{aligned} \tag{9}$$

Normalization using the time-dependent $N_\alpha(x_0(t))$ is allowed here since we assume that the instability develops much faster than noticeable changes occur in $N_\alpha(x_0)$. We seek for perturbations in the vortex and antivortex densities of the form

$$n_\alpha = n_\alpha^{(0)} + f_\alpha \exp[\lambda\tau + ik\zeta + p_\alpha(\xi - \xi_0(\tau))]. \tag{10}$$

The linearized boundary conditions should be written on the perturbed interface,

$$\xi = \xi_0(\zeta, \tau) = \xi_0(\tau) + \delta\xi \exp(ik\zeta + \lambda\tau), \tag{11}$$

with the normal unit vector

$$\vec{\nu} = (1, -ik\delta\xi(\zeta, \tau)). \tag{12}$$

It follows directly from Eq. (6) that

$$\delta\xi = (f_1 - f_2)/2. \tag{13}$$

Equations (1) give the expressions for the parameters p_1 and p_2 . Substituting them and Eqs. (10), (13) into Eqs. (4), (5), we obtain two linear algebraic homogeneous equations relating f_1 and f_2 . Demanding the determinant to vanish and omitting terms of the order of $(Ut_0/L)^2 \ll 1$, one obtains the following dispersion equation for the increment λ at different wave numbers k ,

$$\lambda = \Omega^2 - \epsilon\kappa^2 - 2is\kappa - 1 - b. \tag{14}$$

Here

$$\kappa = \frac{k|\alpha u|}{2}, \quad \alpha = \frac{\gamma_{xy}}{\gamma_{xx}}, \quad u = U\frac{t_0}{L}, \tag{15}$$

$$\epsilon = 4\varepsilon/(\alpha u)^2, \quad s = \text{sign}(\alpha u), \quad 2b = -n_1'' - n_2'',$$

and Ω is a root with $\text{Re}\Omega > 0$ of the equation

$$\begin{aligned} &\Omega^4 + 3\Omega^3 + \Omega^2(-\epsilon\kappa^2 + 2 - 2b) \\ &-\Omega(2\epsilon\kappa^2 + \text{i}s\kappa + 4b) - 3s\text{i}\kappa = 0. \end{aligned} \quad (16)$$

Shown in Fig. 2 is the dependence of the increment $\text{Re}\lambda$ on the dimensionless wave number κ for different ϵ . The parameter b is set to unity as this follows from the quasi-stationarity condition $u \rightarrow 0$. The curves demonstrate that a positive increment exists, i.e. the planar interface becomes unstable, when $\epsilon < \epsilon_c = 0.019$. The instability occurs at not too small values of the anisotropy and velocity of the flux-antiflux interface. Furthermore, it is characterised by a temporal scale given by the largest $\text{Re}\lambda$, λ_m , which occurs at finite $\kappa = \kappa_m$. For ϵ sufficiently small, κ_m is much greater than unity and one finds from Eq. (16)

$$\lambda_m = 1/(4\sqrt{\epsilon}) - 2, \quad \kappa_m = 1/\sqrt{2}\epsilon^{3/4}. \quad (17)$$

Thus, we have identified that an instability occurs if $\epsilon < \epsilon_c$, which in dimensional notation is expressed as

$$\varepsilon < \epsilon_c \left[\frac{U \tan \theta}{2RN_1(x_0)} \right]^2 \quad (18)$$

where θ is the angle between the direction of flux guiding and the flux-antiflux interface. The above analysis allows us to understand why the instability of the vortex-antivortex interface has been observed only in crystals of the 1-2-3 system, where a pronounced guiding effect is expected due to the twin boundaries.

As an illustration we show in Fig. 3 turbulent behaviour observed in an optimally doped YBCO single crystal containing a substantial amount of twinning, see (a). The crystal has a rectangular shape in the **ab** plane and measures 1 mm along the longest edge. Shown in (b) is the MO-image of flux penetration in an external field of 100 mT applied after zero-field-cooling to 45 K. One sees that the field penetrates predominantly from some large twin boundaries located at the bright core of the lines that make 45°-angles with the edges of the crystal. The dark area in the centre of the sample is the region not being penetrated

by a 100 mT applied field at this temperature. In (c) the temperature is raised to 67 K, and the MO-image was recorded in the remanent state after first applying 100 mT. The bright "aura" around the crystal is here the return field of the flux trapped in the central part. Note that this reverse field partly penetrates the sample near the edge. A distinct line can be seen as a dark band going around the crystal just on the inside of the edge. This band is the annihilation zone, which divides the crystal into two opposite magnetic domains. The macroturbulence is here seen as a meandering of the annihilation zone. Adjacent to the zone one can find small areas with increased flux density, see magnified view in (d). Time resolved measurements show that the zone develops in a highly dynamic manner where abrupt redistributions of flux often occur. By adding an external reverse field to the remanent state the annihilation zone is pushed further into the crystal and the dynamical features becomes even more spectacular.

In this crystal the turbulent behavior was observed in the interval 25-75 K. As the temperature increases the dynamics of the flux/antiflux interface becomes increasingly rapid. However, above 75 K there again appears to be no irregular behavior of the interface.

The existence of the instability only in a definite temperature region finds a simple rationalization within our model. At low temperatures, the viscosity increases exponentially, and the characteristic spatial scale L , in Eq. (9), decreases correspondingly and becomes comparable to or less than the twin-boundary spacing. As a result, the guiding effect is suppressed and the instability disappears. On the other hand, at temperatures close to T_c the flux guiding is no longer effective due to thermal activation of the vortices. It is remarkable, and in full support of our model, that in the present heavily twinned crystal the turbulence occurs down to much lower temperatures than found in previous studies of similar crystals with only little twinning [11,3].

In conclusion, we have presented a theoretical model which gives a fully consistent description of the macroturbulence phenomenon we observe in HTS materials under certain conditions. This work is supported by INTAS/RFBR and RFBR, grants IR-97-1394 and 00-02-17145, 00-02-18032, and the Research Council of Norway.

REFERENCES

- [1] V.K. Vlasko-Vlasov, V.I. Nikitenko, A.A. Polyanskii, G.W. Grabtree, U. Welp, and B.W. Veal, *Physica C* **222**, 361 (1994).
- [2] M.V. Indenbom, Th. Schuster, M.R. Koblishka, A. Forkl, H. Kronmüller, L.A. Dorosinskii, V.K. Vlasko-Vlasov, A.A. Polyanskii, R.L. Prozorov, and V.I. Nikitenko, *Physica C* **209**, 259 (1993).
- [3] T. Frello, M. Baziljevich, T.H. Johansen, N.H. Andersen, Th. Wolf, and M.R. Koblishka, *Phys. Rev. B* **59**, R6639 (1999).
- [4] C.P. Bean, *Phys. Rev. Lett.* **8**, 250 (1962).
- [5] Y. Yeshurun, A.P. Malozemoff, and A. Shaulov, *Rev. Mod. Phys.* **68**, 911 (1996).
- [6] F. Bass, B.Ya. Shapiro, I. Shapiro, and M. Shvartsner, *Phys. Rev. B* **58**, 2878 (1998).
- [7] The ratio of the core energy and magnetic energy of a vortex is $W_c/W_J \approx H_{c1}^2/H_{c2}H_0 \ll 1$ (H_{c1} and H_{c2} are the lower and upper critical magnetic fields, and H_0 is the magnetic field on the sample surface). Release of the core energy of all vortices in the sample would increase the temperature only on the order of 10^{-4} K.
- [8] A.K. Niessen, C.H. Weijsenfeld, *J. Appl. Phys.*, **40**, 384 (1969).
- [9] H. Pastoriza, S Candia, G. Nieva, *Phys. Rev. Lett.* , **83**, 1026 (1999).
- [10] L.D. Landau and E.M. Lifshits, *Fluid Mechanics* (Butterworth-Heinemann, Oxford, 1987).
- [11] M.R. Koblishka, T.H. Johansen, M. Baziljevich, H. Hauglin, H. Bratsberg and B.Ya. Shapiro, *Europhys. Lett.* **41**, 419 (1998).

FIGURES

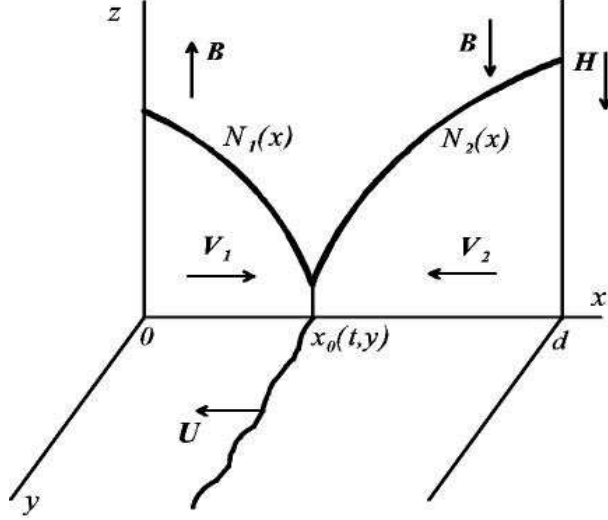


FIG. 1. Flux distribution in one half of an infinite slab ($|x| \leq d$) containing trapped vortices of density $N_1(x)$ in the central region $|x| \leq x_0$, and antivortices of density $N_2(x)$ penetrating from the outside. The other symbols are defined in the text.

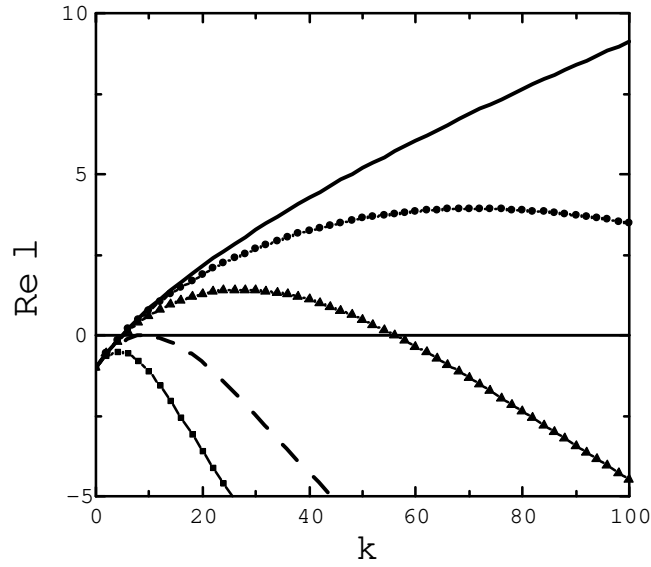


FIG. 2. The dependence $\text{Re}\lambda(\kappa)$ at different anisotropy parameters ε : $\varepsilon = 0$ (solid line), $\varepsilon = 0.0015$ (circles), $\varepsilon = 0.005$ (triangles), $\varepsilon = \varepsilon_c = 0.019$ (dashed line), $\varepsilon = 0.05$ (boxes).

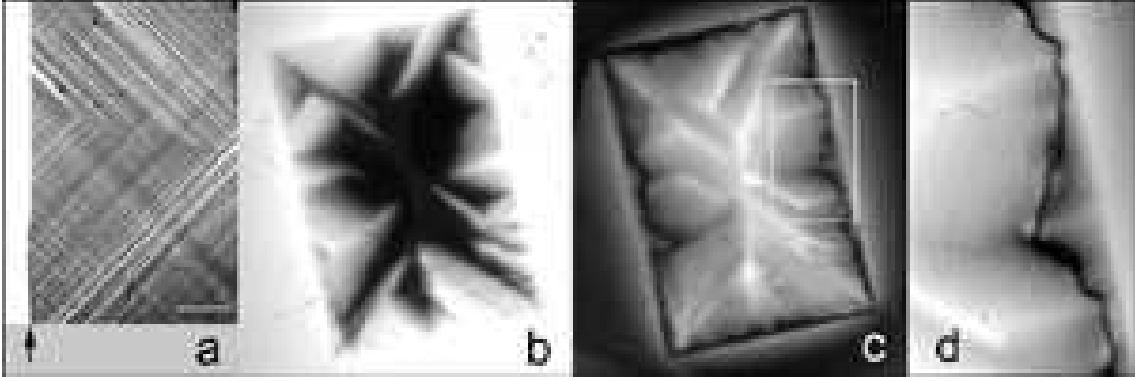


FIG. 3. (a) - Polarized light image showing twin domains in a small area on the crystal. The arrow indicates the sample edge, and the scale bar is $50 \mu\text{m}$ long. (b)-(d) are magneto-optical images where the brightness represents the magnitude of \mathbf{B} 's component normal to the surface. (b) - Applied field of $B_a = 100 \text{ mT}$ at $T = 45 \text{ K}$. (c) - Remanent state after full flux penetration at $T = 67 \text{ K}$. (d) - magnified view of the area marked in (c)